Molecular Pharmacology Fast Forward. Published on March 9, 2017 as DOI: 10.1124/mol.116.106419
This article has not been copyedited and formatted. The final version may differ from this version.

MOLPHARM/2016/106419

Title page:

Purinergic receptor transactivation by the β_2-adrenergic receptor increases intracellular Ca^{2+} in non-excitable cells.

Wayne Stallaert, Emma T van der Westhuizen, Anne-Marie Schönegge, Bianca Plouffe, Mireille Hogue, Viktoria Lukashova, Asuka Inoue, Satoru Ishida, Junken Aoki, Christian Le Gouill & Michel Bouvier.

Department of Biochemistry, Université de Montréal, Montréal, QC, Canada (WS, ETvdW, A-MS, BP, MB). Institute for Research in Immunology and Cancer, Université de Montréal, Montréal, QC, Canada (WS, ETvdW, A-MS, BP, MH, VL, CLG, MB). Monash Institute for Pharmaceutical Sciences, Monash University, Parkville, Victoria, Australia (ETvdW). Graduate School of Pharmaceutical Sciences, Tohoku University, Sendai, Miyagi, Japan (AI, SI, JA). Japan Science and Technology Agency (JST), Precursory Research for Embryonic Science and Technology (PRESTO), Kawaguchi, Saitama, Japan (AI). Japan Agency for Medical Research and Development, Core Research for Evolutional Science and Technology (AMED-CREST), Chiyoda-ku, Tokyo, Japan (JA).

Molecular Pharmacology Fast Forward. Published on March 9, 2017 as DOI: 10.1124/mol.116.106419
This article has not been copyedited and formatted. The final version may differ from this version.

Running title page:

a) Running title: β_2AR transactivation of purinergic receptors

b) Corresponding author: Michel Bouvier, IRIC - Université de Montréal, P.O. Box 6128 Succursale Centre-Ville, Montréal, Qc. Canada, H3C 3J7. Tel: +1-514-343-6319. Fax: +1-514-343-6843. Email: michel.bouvier@umontreal.ca

c)

Number of:	text pages:	37
	tables:	0
	figures:	8
	references:	58
Number of words in:	abstract:	238
	introduction:	572 (max 750)
	discussion:	1029 (max 1500)

d) Non standard abbreviations: 2-APB, 2-aminoethoxydiphenyl borate; AC, adenylyl cylase; β_2AR, β_2 adrenergic receptor; BAPTA-AM, 1,2-Bis(2-aminophenoxy)ethane-N,N,N′,N′-tetraacetic acid tetrakis(acetoxymethyl ester); BRET, bioluminescent resonance energy transfer; Cch, Carbamylcholine chloride; CTX, cholera toxin; EGFR, epidermal growth factor receptor; FRET, fluorescent resonance energy transfer; HB-EGF, heparin-binding epidermal growth factor; HEK293, human embryonic kidney 293cells; TG, thapsigargin;

Molecular Pharmacology Fast Forward. Published on March 9, 2017 as DOI: 10.1124/mol.116.106419
This article has not been copyedited and formatted. The final version may differ from this version.

Abstract:

The β_2 adrenergic receptor (β_2AR) increases intracellular Ca^{2+} in a variety of cell types. By combining pharmacological and genetic manipulations, we reveal a novel mechanism through which the β_2AR promotes Ca^{2+} mobilization ($pEC_{50} = 7.32 \pm 0.10$) in non-excitable human embryonic kidney (HEK)-293S cells. Down-regulation of Gs with sustained cholera toxin pre-treatment and the use Gs-null HEK293 (ΔGs-HEK293) cells generated using the CRISPR/Cas9 system, combined with pharmacological modulation of cAMP formation revealed a Gs-dependent but cAMP-independent increase in intracellular Ca^{2+} following β_2AR stimulation. The increase in cytoplasmic Ca^{2+} was inhibited by P2Y purinergic receptor antagonists as well as a dominant negative mutant form of Gq, a Gq-selective inhibitor and an IP_3 receptor antagonist, suggesting a role for this Gq-coupled receptor family downstream of the β_2AR activation. Consistent with this mechanism, β_2AR stimulation promoted the extracellular release of adenosine triphosphate (ATP) and pre-treatment with apyrase inhibited the β_2AR-promoted Ca^{2+} mobilization. Together, these data support a model whereby the β_2AR stimulates a Gs-dependent release of ATP, which transactivates Gq-coupled P2Y receptors through an "inside-out" mechanism, leading to a Gq- and IP_3-dependent Ca^{2+} mobilization from intracellular stores. Given that β_2AR and P2Y receptors are co-expressed in various tissues, this novel signalling paradigm could be physiologically important and have therapeutic implications. In addition, this study reports the generation and validation of HEK293 cells deleted of Gs using the CRISPR/Cas9 genome editing technology that will undoubtedly be powerful tools to study Gs-dependent signalling.

Molecular Pharmacology Fast Forward. Published on March 9, 2017 as DOI: 10.1124/mol.116.106419
This article has not been copyedited and formatted. The final version may differ from this version.

Introduction:

The β_2 adrenergic receptor (β_2AR) has been shown to regulate a vast signalling network, leading to the activation of key cellular effectors such as adenylyl cyclase (AC), ERK1/2 and Akt (De Blasi, 1990; Daaka et al., 1998; Bommakanti et al., 2000) to control a variety of physiological processes, including the regulation of cardiac function, smooth muscle tone, immunological responses, fat metabolism as well as both central and peripheral nervous system activity (Guimaraes and Moura, 2001; Collins et al., 2004; Sitkauskiene and Sakalauska, 2005; Pérez-Schindler et al., 2013). Although much is known about the signalling repertoire of the β_2AR, new insights into its full signalling capabilities and its role in cellular biology continue to be discovered (Stallaert et al., 2012; van der Westhuizen et al., 2014).

In addition to the abovementioned signalling pathways, the β_2AR can also stimulate an increase in intracellular Ca^{2+}. This signalling response is well established in excitable cells, such as cardiomyocytes, via a mechanism involving cAMP-mediated regulation of plasma membrane L-type Ca^{2+} channels (Zhang et al., 2001; Christ et al., 2009; Benitah et al., 2010). However, increases in intracellular Ca^{2+} levels have also been observed in non-excitable cells, such as alveolar epithelial cells (Keller et al., 2014) and in human embryonic kidney cells (HEK293) endogenously or stably overexpressing the β_2AR (Schmidt et al., 2001; Stallaert et al., 2012; van der Westhuizen et al., 2014). Previous observations from our laboratory indicated that such β_2AR-mediated increases in intracellular Ca^{2+} in HEK293 cells are inhibited by an IP_3 receptor antagonist, 2-aminoethoxydiphenyl borate (2-APB) (Stallaert et al., 2012), suggesting the release of Ca^{2+} from intracellular stores, which points to a mechanism distinct from the plasma membrane Ca^{2+} channel activation described in excitable cells.

Molecular Pharmacology Fast Forward. Published on March 9, 2017 as DOI: 10.1124/mol.116.106419
This article has not been copyedited and formatted. The final version may differ from this version.

Several studies have reported that activation of the β_2AR can also stimulate the release of extracellular mediators as part of its signalling repertoire. Activation of the β_2AR in mouse skeletal muscle, vascular smooth muscle cells or cardiac fibroblasts promotes the extracellular release of cAMP, which is converted to AMP by ecto-phosphodiesterases and then to adenosine by ecto-5'-nucleotidase on the extracellular surface of the cells (Dubey et al., 1996; 2001; Duarte et al., 2012). In addition, extracellular adenosine can be produced by the release of intracellular adenine nucleotides to the extracellular space, which are converted to adenosine by ecto-ATPase, ecto-ADPase and ecto-5'-nuclotidase (Jackson et al., 1996). Stimulation of human erythrocytes with isoproterenol (ISO) increases extracellular ATP levels (Montalbetti et al., 2011), suggesting that βARs can also be coupled to ATP release. In some cases, this release of mediators into the extracellular milieu can lead to the subsequent transactivation of other GPCRs or receptor tyrosine kinases. Previously, an "inside-out" signalling mechanism was demonstrated for the β_2AR, leading to the transactivation of adenosine receptors through the production of extracellular adenosine as described above (Sumi et al., 2010), as well as the epithelial growth receptor (EGFR) through the membrane shedding of heparin-binding epithelial growth factor (HB-EGF) (Kim et al., 2002).

In this study, we describe a new "inside-out" pathway activated by the β_2AR in non-excitable cells, involving the Gs-dependent, but cAMP-independent increase in intracellular Ca^{2+} through the release of extracellular ATP and the subsequent transactivation of Gq-coupled P2Y purinergic receptors, providing a previously unrecognised link between adrenergic and purinergic receptors. This study also provides the first description and use of CRISPR/Cas9 genomic editing to knockout Gs in human cells, providing a powerful new tool to explore the signalling events downstream of this Gα subunit.

Molecular Pharmacology Fast Forward. Published on March 9, 2017 as DOI: 10.1124/mol.116.106419
This article has not been copyedited and formatted. The final version may differ from this version.

Materials and Methods:

Reagents: (-)-isoproterenol hydrochloride (ISO), carbamoylcholine chloride (Cch), thapsigargin (TG), 8-bromo-cAMP (8-br-cAMP), forskolin, cholera toxin (CTX), , suramin and apyrase were purchased from Sigma Aldrich (St. Louis, MO, USA). ICI118,551, 1,2-Bis(2-aminophenoxy)ethane-N,N,N',N'-tetraacetic acid tetrakis(acetoxymethyl ester) (BAPTA-AM), 2-aminoethoxydiphenyl borate (2-APB), 9-(Tetrahydro-2-furanyl)-9H-purin-6-amine (SQ22536), , 8,8'-[Carbonyl*bis*[imino-3,1-phenylenecarbonylimino(4-fluoro-3,1-phenylene)carbonylimino]]*bis*-1,3,5-naphthalenetrisulfonic acid hexasodium salt (NF157), 4,4'-(Carbonyl*bis*(imino-3,1-(4-methyl-phenylene)carbonylimino))*bis*(naphthalene-2,6-disulfonic acid) tetrasodium salt (NF340), 8,8'-[Carbonyl*bis*(imino-4,1-phenylenecarbonylimino-4,1-phenylenecarbonylimino)]*bis*-1,3,5-naphthalenetrisulfonic acid hexasodium salt (NF279), *N*-Cyano-*N*''-[(1*S*)-1-phenylethyl]-*N*'-5-quinolinyl-guanidine (A-804598), 5-(3-Bromophenyl)-1,3-dihydro-2*H*-benzofuro[3,2-*e*]-1,4-diazepin-2-one (5-BDBD), 9-Chloro-2-(2-furanyl)-[1,2,4]triazolo[1,5-c]quinazolin-5-amine (CGS 15943) and 4,4',4'',4'''-[Carbonylbis(imino-5,1,3-benzenetriyl-bis(carbonylimino))]tetrakis-1,3-benzenedisulfonic acid octasodium salt (NF449) were obtained from R&D Systems (Minneapolis, MN, USA). Coelenterazine 400a and coelenterazine h were purchased from Nanolight technologies (Pinetop, AZ, USA) and coelenterazine cp was purchased from Biotium (Hayward, CA, USA). Arginine-vasopressine (AVP) and 5-(Methylamino)-2-[[2*R*,3*R*,6*S*,8*S*,9*R*,11*R*) -3,9,11-trimethyl-8-[(1*S*)-1-methyl-2-oxo-2-(1*H*-pyrrol-2-yl)-ethyl]-1,7-dioxaspiro[5.5]undec-2-yl]methyl]-4-benzoxazolecarboxylic acid (A23187) were from Tocris (Bio-Techne, Minneapolis, MN, USA). Cell culture reagents were from Wisent Incorporated (Montreal, QC, Canada). The Gq selective inhibitor, FR900359 (Schrage et al., 2015) was obtained from Dr. Eve Kostenis and Dr. Stefan Kehraus from the

Molecular Pharmacology Fast Forward. Published on March 9, 2017 as DOI: 10.1124/mol.116.106419
This article has not been copyedited and formatted. The final version may differ from this version.

University of Bonn. The Gq and Gq(Q209L/D277N) constructs were purchased from Missouri S&T cDNA Resource Center (Rolla, MO, USA). Hap II, Pvu II and Hae II restriction enzymes were from Takara Bio (Japan). All other reagents were obtained from Sigma-Aldrich unless otherwise stated.

Cell culture and transfections: Parental HEK293S cells or HEK293S cells stably expressing an amino-terminal tagged human β_2AR (3.17 ± 0.32 pmol/mg protein; HA-β_2AR-HEK293S cells; Galandrin et al. 2006) were grown at 37°C with 5% CO_2 in Dulbecco's modified Eagle's medium (DMEM) supplemented with 5% fetal bovine serum. HEK293S and HA-β_2AR-HEK293S cells were transiently transfected (600 000 cells/well) in 6 well plates with biosensors (950 ng/1×10^6 cells) for Ca^{2+} measurements (Obelin luminescence), bioluminescence resonance energy transfer (BRET) and fluorescence resonance energy transfer (FRET) assays using linear polyethylenimine (PEI; 1 mg/ml; Polysciences Inc., Warrington, PA) diluted in NaCl (150 mM, pH 7.0) (PEI:DNA ratio 3:1) as previously described (Reed et al., 2006). Twenty four hours post-transfection, cells were re-plated (50,000 cells/well) onto white 96-well CulturePlates (Perkin-Elmer, Woodbridge, ON, Canada). Six hours after re-plating, growth medium was replaced with fresh starvation media consisting of DMEM supplemented with 0.5% FBS for the next 18 h.

Parental HEK293 and ΔGs-HEK293 cells were cultured and transfected as described for the HEK293S cells, with the following modification: medium was supplemented with 10% FBS, PEI was diluted in Dulbecco's Phosphate-Buffered Saline (DPBS) and added to cells in suspension (300,000-350,000 cells/ml). Cells were then transferred into white 96-well CulturePlates (30,000-35,000 cells/well). Cells were cultured with 10% FBS for the following 48 hrs prior to experimentation.

Molecular Pharmacology Fast Forward. Published on March 9, 2017 as DOI: 10.1124/mol.116.106419
This article has not been copyedited and formatted. The final version may differ from this version.

Generation of HEK293 cells devoided of Gs (ΔGs-HEK293): The two members (Gαs and Gαolf, encoded by the *GNAS* and the *GNAL* genes, respectively; both were expressed in HEK293 cells) of the Gαs family were simultaneously targeted by a CRISPR/Cas9 system to introduce frame shift into the coding sequence as described previously (Ran, et al., 2013) with some modifications. Briefly, *GNAS*-targeting sgRNA sequence (5'-CTACAACATGGTCATCCGGG-3') was inserted into the Bbs I site of the pSpCas9(BB)-2A-GFP vector (PX458; a gift from Feng Zhang, Broad Institute; Addgene plasmid # 48138) using two synthesized oligonucleotides (5'-CACCGCTACAACATGGTCATCCGGG-3' and 5'-AAACCCCGGATGACCATGTTGTAGC-3'; FASMAC, Japan). Similarly, *GNAL*-targeting sgRNA sequence #1 (5'-TGTTTGATGTTGGTGGCCAG-3'), #2 (5'-GTAATGTTTGCCGTCACCGG-3') and #3 (5'-ATTGTGCACAGTCAATCAGC-3') were inserted using three sets of oligonucleotides (for #1, 5'-CACCGTGTTTGATGTTGGTGGCCAG-3' and 5'-AAACCTGGCCACCAACATCAAACAC-3'; for #2, 5'-CACCGTAATGTTTGCCGTCACCGG-3' and 5'-AAACCCGGTGACGGCAAACATTAC-3'; for #3, 5'-CACCGATTGTGCACAGTCAATCAGC-3' and 5'-AAACGCTGATTGACTGTGCACAATC-3'). Correct insertion of the sgRNA sequences was verified by sequencing using the Sanger method (FASMAC, Japan). HEK293 (200,000 cells/well) were seeded into 12 well plates and transfected with a mixture of the *GNAS*-targeting PX458 vectors and either of the *GNAL*-targeting PX458 vectors (0.25 μg each/well) with Lipofectamine® 2000 (Life Technologies, CA, USA). Twenty four hours later, cells were detached and GFP-positive cells (approximately 30% of cells) were isolated using a cell sorter (SH800, Sony, Japan). After growing clonal cell colonies, clones were analyzed for mutations in the *GNAS* and the *GNAL* genes by PCR and

Molecular Pharmacology Fast Forward. Published on March 9, 2017 as DOI: 10.1124/mol.116.106419
This article has not been copyedited and formatted. The final version may differ from this version.

restriction enzyme digestion, using the primer and restriction enzyme combinations shown in Supplemental Table 1. PCR was performed with an initial denaturation cycle of 95ºC for 2 min, followed by 35 cycles of 95ºC for 15 sec, 64ºC for 30 sec and 72ºC for 30 sec. The resulting PCR product was digested with the corresponding restriction enzyme and analyzed by agarose gel electrophoresis. Candidate positive clones were further analyzed by genomic DNA sequencing using a TA cloning method. The lack of functional Gs was also confirmed by assessing GPCR-stimulated cAMP production as described below. For the TA cloning, PCR-amplified genomic DNA fragments using an ExTaq polymerase (Takara Bio, Japan) were gel-purified (Promega, WI, USA) and cloned into a pMD20 T-vector (Takara Bio, Japan). Ligated products were introduced into SCS1 competent cells (Stratagene, CA, USA) and transformed cells were selected on an ampicillin-containing LB plate. At least twelve colonies were picked and inserted fragments were PCR-amplified using the ExTaq polymerase and primers (5'-CAGGAAACAGCTATGAC-3' (M13 Primer RV) and 5'-GTTTTCCCAGTCACGAC-3' (M13 Primer M4)) designed to anneal the pME20 T-vectors. PCR products of the transformed pMD20 T-vector were sequenced using the Sanger method (FASMAC, Japan) and the M13 Primer RV.

Whole transcriptome expression profiling was performed using the Clariom S assay (human, analysis using the Transcriptome Analysis Console from Affymetrix) to assess differences in gene expression between the parental HEK293 and ΔGs-HEK293 cell lines (Supplemental Figure 5 and Supplemental Tables 2 and 3).

***mRNA expression*:** Total RNA was isolated from $3x10^6$ HA-β_2AR-HEK293S cells using the RNAeasy Mini kit (QIAGEN, Hilden, Germany) according to the manufacturer's protocol for animal cells. Microarray analysis of mRNA samples was performed using Illumina's HumanRef-8 v3.0 expression bead chips at McGill University and the Génome Québec Innovation Centre.

Molecular Pharmacology Fast Forward. Published on March 9, 2017 as DOI: 10.1124/mol.116.106419
This article has not been copyedited and formatted. The final version may differ from this version.

The gene expression microarray data was analyzed and normalized by the bioinformatics platform at the Institute for Research in Immunology and Cancer (IRIC) at the University of Montreal. The raw fluorescent values were then normalized using a quantile normalization method (Bolstad et al., 2003; Lemieux, 2006), which re-ranks the sampled based on the raw fluorescent values obtained for each probe. Using this method of normalization, the distribution of the samples becomes the reference point, therefore, no internal control is required. For the microarray dataset analyzed, the distribution of the data is defined by the median value 7.162; the minimum value 5.851 and the maximum value 15.760, the first quartile of 6.578 and the third quartile of 9.215. The normalized values were plotted alongside known housekeeping genes, β-actin and α-tubulin, which were used for comparison purposes to represent genes that are highly expressed in the cells. The inhibitory G protein, Gαo, was also plotted because it is not expressed in HEK293 cells (Law et al., 1993) and therefore represents an appropriate baseline background value.

Western blot analysis: The parental HEK293 cells and the ΔGs-HEK293 cells were harvested and approximately 1 x 10^6 cells were lysed in 500 µL of SDS-PAGE sample buffer (62.5 mM Tris-HCl (pH 6.8), 50 mM dithiothreitol, 2% SDS, 10% Glycerol and 4 M urea) containing 1 mM EDTA and 1 mM phenylmethylsulfonyl fluoride. Cell lysates were homogenized with a handy ultrasonic homogenizer (Microtech) and boiled at 95ºC for 5 min. Western blots were performed according to standard procedures using an anti-G α s/olf mouse monoclonal antibody (clone E-7, cat. no. sc55546, Santa Cruz Biotechnology) or anti-α-tubulin mouse monoclonal antibody (clone DM1A, cat. no. sc-32293, Santa Cruz Biotechnology) (both at 1 µg/mL in Tris-buffered saline, 1% BSA and 0.05% Tween 20), followed by horse radish peroxidase-linked anti-mouse IgG secondary antibody (cat. no. NA9310, GE Healthcare; 1:2000 diluted with Tris-

Molecular Pharmacology Fast Forward. Published on March 9, 2017 as DOI: 10.1124/mol.116.106419
This article has not been copyedited and formatted. The final version may differ from this version.

buffered saline, 5% skim milk, 0.05% Tween 20). Chemiluminescence signals were detected using a LAS-4000 (FujiFilm) and visualized with Multi Gauge ver. 3.0 (FujiFilm).

Ca^{2+} measurements: Ca^{2+} measurements were carried out as described previously (van der Westhuizen et al., 2014). Briefly, HEK293S, HA-β_2AR-HEK293S or ΔGs-HEK293 cells were transiently transfected with the mCherry-obelin or GFP2-obelin-based Ca^{2+}-sensitive biosensors. The day of experimentation, cells were washed twice and pre-incubated in stimulation buffer (Modified Hank's Balances Salt Solution (HBSS): 137 mM NaCl, 5.4 mM KCl, 0.25 mM Na_2HPO_4, 0.44 mM KH_2PO_4, 1.8 mM $CaCl_2$, 0.8 mM $MgSO_4$, 4.2 mM $NaHCO_3$, 0.2% (w/v) D-glucose, pH 7.4) containing the obelin substrate, coelenterazine cp (1 μM), at 25°C for 2 h in the dark. Compounds diluted in stimulation buffer were injected into the wells and luminescence readings were taken every 0.3 seconds using the SpectraMax L (Molecular Devices, Sunnyvale, CA). Luminescence was monitored for a total of 60 seconds post-stimulation and expressed as relative luminescence units (RLU). The area under the resulting curves (AUC) and the peak response to stimulation were calculated. Where indicated, the AUC was transformed as % peak ISO or A23187 response.

cAMP production: cAMP production measurements were carried out as described previously (van der Westhuizen et al., 2014). Briefly, cells were transfected as indicated with either the FRET-based GFP10-EPAC1-vYFP or the BRET-based GFP_{10}-EPAC1-RlucII cAMP-sensitive biosensors in which binding of cAMP induces a conformational change that leads to a decrease in FRET or BRET. Compounds were diluted in stimulation buffer and added to cells at 37°C for 30 minutes prior to measurement. The light emitted from FRET donor and acceptor proteins was measured with the FlexStation II (Molecular Devices, Sunnyvale, CA, USA) using the 510 nm (GFP_{10}) and 533 nm (vYFP) emission filters. BRET was measured with the Mithras LB 940

Molecular Pharmacology Fast Forward. Published on March 9, 2017 as DOI: 10.1124/mol.116.106419
This article has not been copyedited and formatted. The final version may differ from this version.

(Berthold Technologies, Bad Wildbad, Germany) using 410±70 nm (RlucII) and 515±20 nm (GFP_{10}) emission filters or the SynergyNeo microplate reader from BioTek using 410±80 nm and 515±30 nm emission filters. FRET or BRET ratios were calculated (acceptor/donor) and ΔFRET and ΔBRET were determined by subtracting the FRET or BRET signal generated in vehicle treatment control conditions.

Measurements of cAMP for Figure 4A were performed using the HTRF-cAMP dynamic kit (Cisbio) as described previously (Stallaert et al., 2012).

***Gs activation assay*:** HA-β_2AR-HEK293S cells were co-transfected with a three-component G protein activation biosensor composed of Gαs-67-RlucII (50 ng/well), Gβ1 (100 ng/well) and GFP_{10}-Gγ1 (100 ng/well) in which Gs activation results in the separation between the Gα and Gβγ subunits, thus leading to a decrease in BRET (Gales et al., 2005). The day of the experiment, cells were washed twice with stimulation buffer and pre-treated with various inhibitors diluted in stimulation buffer for the indicated times at 37°C. Coelenterazine 400a, diluted in stimulation buffer (5 µM) was added to the wells for 5 min, then increasing concentrations of ISO were added for 2 min. Plates were read on the Mithras LB 940 with 410±70 nm (RlucII) and 515±20 nm (GFP_{10}) emission filters and BRET ratios calculated as above.

Quantification of extracellular ATP: Extracellular ATP was measured using the luciferin-luciferase-based ENLITEN® ATP Assay System (Promega, Madison, WI, USA) according to the manufacturer's instructions. Briefly, cells were grown to 90-100% confluence in a 96-well plate. Cells were washed with stimulation buffer, then pre-treated with 10 µM ICI 118,551 or stimulation buffer (vehicle) for 30 min at 37°C. Cells were stimulated with 10 µM ISO and the cell supernatant (conditioned buffer) was collected at 15-120 sec post stimulation. Luciferin-

Molecular Pharmacology Fast Forward. Published on March 9, 2017 as DOI: 10.1124/mol.116.106419
This article has not been copyedited and formatted. The final version may differ from this version.

luciferase reagent (100 µl) was injected into 10 µl of conditioned buffer, and luminescence was measured on the Mithras LB 940 (Berthold Technologies, Bad Wildbad, Germany). ATP concentration of each sample was determined by comparing the luminescence of samples with those of standards in the concentration range of 10^{-6} to 10^{-10} M.

***Data Analysis*:** Data analysis was performed using Microsoft Excel (Microsoft, Redmond, WA, USA) and GraphPad Prism (versions 5 and 6, GraphPad Software, La Jolla, CA, USA). Statistical analyses were performed as indicated in Figure legends.

Molecular Pharmacology Fast Forward. Published on March 9, 2017 as DOI: 10.1124/mol.116.106419
This article has not been copyedited and formatted. The final version may differ from this version.

Results:

β_2AR activation leads to an increase in intracellular Ca^{2+} in HEK293S cells: Isoproterenol (ISO) stimulation of the endogenously expressed β_2ARs in HEK293S cells induces a rapid and transient increase in intracellular Ca^{2+} (Figure 1A). The increase in intracellular Ca^{2+} was detected as early as 5 seconds following the addition of ISO, reaching a maximum at approximately 12 seconds followed by a slow decrease thereafter and returning to basal levels 60 seconds post-stimulation, demonstrating a functional Ca^{2+} response in non-excitable cells that endogenously express the receptor. Stable overexpression of the β_2AR in HEK293S cells (HA-β_2AR-HEK293S cells) led to acceleration in the onset (≈ 2 sec) and increased magnitude of the response (Figure 1B). This increase in intracellular Ca^{2+} was inhibited in both cell lines following pre-treatment with the β_2AR-selective antagonist, ICI 118,551, confirming the β_2AR-specificity of the response (Figure 1C). The response was concentration-dependent, yielding similar pEC_{50} values for ISO in both cell lines (7.32±0.10 and 7.05±0.16 in HEK293S and HA-β_2AR-HEK293S cells, respectively) (Figure 1D).

β_2AR promotes a Gs-dependent but cAMP-independent Ca^{2+} response: To probe the mechanism underlying the β_2AR-mediated Ca^{2+} response, we first examined the Gs/cAMP pathway in the HA-β_2AR-HEK293S cell line, which produces a larger Ca^{2+} response following stimulation, thus facilitating its mechanistic dissection. To confirm the involvement of Gs, the primary G protein-coupling partner of the β_2AR, we tested the effect of overnight pre-treatment with cholera toxin (CTX) to down-regulate Gs signalling (Levis and Bourne, 1992), as well as the effect of acute pre-treatment with a small molecule inhibitor of Gs, NF449 (which prevents GDP/GTP exchange (Hohenegger et al., 1998)). We found that the ISO-stimulated Ca^{2+} response was significantly inhibited by both CTX and NF449 pre-treatment (Figure 2A), suggesting the

Molecular Pharmacology Fast Forward. Published on March 9, 2017 as DOI: 10.1124/mol.116.106419
This article has not been copyedited and formatted. The final version may differ from this version.

involvement of Gs in the β_2AR-mediated Ca^{2+} response. However, while chronic pre-treatment with CTX led to the expected inhibition of Gs activation measured using a bioluminescence resonance energy transfer (BRET)-based biosensor that monitors the separation between Gαs and Gγ1 as a reporter for G protein activation (Gales et al., 2005), acute pre-treatment with NF449 had no impact on Gs activation (Figure 2B), indicating that its effect on the β_2AR-promoted Ca^{2+} response resulted from another mechanism of action. This is consistent with the fact that, although a potent and selective inhibitor of Gαs, NF449 contains multiple negative charges (El-Ajouz et al., 2012) that impede its cell permeability and likely restrict its effect to extracellular target(s) in cell-based assays. Observations that NF449 is also a potent antagonist of purinergic P2X and P2Y receptors (Braun et al., 2001; Kassack et al., 2004) provided valuable insights into additional mechanistic components underlying the β_2AR-stimulated Ca^{2+} response, as discussed below. However, the inhibitory effect of sustained CTX treatment supported a role for Gs in the Ca^{2+} response.

To confirm the role of Gs in the cytoplasmic Ca^{2+} increase, we genetically deleted functional Gs from HEK293 cells using the CRISPR/Cas9 system (ΔGs-HEK293). The genetic characterization of three ΔGs cell clones is presented in Supplemental Figures 1-4. Loss of both the long (GαsL) and the short (GαsS) forms of Gαs was confirmed in 3 ΔGs-HEK293 clones (Figure 2C).

ΔGs cells were then tested for a loss of function using the BRET-based EPAC biosensor to monitor the effect of Gs knockout on the β_2AR-mediated cAMP response. In ΔGs-HEK293 cells, the cAMP response to ISO stimulation was significantly reduced compared to parental HEK293 cells (Figure 2D, Supplemental Figure 4A). Similarly, stimulation of another Gs-coupled receptor, the vasopressin type 2 receptor, with AVP failed to promote cAMP accumulation in all

Molecular Pharmacology Fast Forward. Published on March 9, 2017 as DOI: 10.1124/mol.116.106419
This article has not been copyedited and formatted. The final version may differ from this version.

3 ΔGs-HEK293 selected clones (Supplemental Figure 4B). Furthermore, the ISO-promoted increase in intracellular Ca^{2+} was also found to be inhibited in ΔGs-HEK293 cells (Figure 2E, Supplemental Figure 4C), while the response to the Ca^{2+} ionophore, A23187, was similar to that observed in parental HEK293 cells (Figure 2F, Supplemental Figure 4C), thus confirming the essential role of Gs in the β_2AR-promoted Ca^{2+} response. The loss of Ca^{2+} responses to β_2AR stimulation was observed in all 3 ΔGs-HEK293 clones (Supplemental Figure 4C), excluding a possible clonal effect. Furthermore, a gene array analysis (Supplemental Figure 5) of the parental and one of the ΔGs-HEK293 cells (clone 1) revealed that none of the other G protein subunit (α, β or γ) were among the 489 genes (out of 21,448 genes detected) found to be significantly up or down regulated with a minimum threshold of 2 fold in the ΔGs cells (Supplemental Table 2), excluding the possible implication of other G protein expression changes in the observed responses. The expression level of the G protein subunits detected in the microarray for parental and ΔGs cells are presented in Supplemental Table 3.

We next assessed the role of the Gs-, and adenylate cyclase (AC)-dependent second messenger cAMP in the ISO-promoted Ca^{2+} response. Pre-treatment with SQ22536, a pharmacological inhibitor of AC, significantly inhibited ISO-promoted cAMP production (by 43%; Figure 3A), yet it failed to block the Ca^{2+} response (Figure 3B), producing a response higher than in the absence of the inhibitor. To further confirm this surprising result, we directly assessed whether increases in intracellular cAMP alone were capable of generating a Ca^{2+} response. Stimulation with forskolin (Fsk), which increases cAMP independently of β_2AR activation through the direct activation of AC (Seamon et al., 1981), increased the intracellular cAMP to a similar level as obtained for ISO (Figures 2D and 3C), yet elicited only a marginal Ca^{2+} response (Figure 3D). Further supporting these results, the cell permeable cAMP analog, 8-

Molecular Pharmacology Fast Forward. Published on March 9, 2017 as DOI: 10.1124/mol.116.106419
This article has not been copyedited and formatted. The final version may differ from this version.

bromo-cAMP, elicited a similarly weak Ca^{2+} response (Figure 3E**)**. Taken together, our data indicate the β_2AR-promoted increase in intracellular Ca^{2+}occurs predominantly independently of cAMP production.

Involvement of purinergic receptors in the β_2AR-promoted Ca^{2+} response: To further investigate the above observation that NF449, a small molecule inhibitor of Gs and a purinergic receptor antagonist (Braun et al. 2001; Kassack et al. 2004), blocked the ISO-promoted Ca^{2+} response (see Figure 2A), we assessed additional purinergic receptor antagonists to test the potential role of this receptor family. Pre-treatment with a pan-purinergic receptor antagonist, suramin, significantly inhibited the ISO-promoted increase in intracellular Ca^{2+} (Figure 4A), while the pan-adenosine receptor antagonist CGS 15943 had no effect (Figure 4B). Gene expression microarray analysis of HA-β_2AR-HEK293S cells indicated the expression of several P2X purinergic ion channels and P2Y purinergic GPCRs in this cell line (Supplemental Figure 6). To determine the identity of the purinergic receptor(s) involved in the Ca^{2+} response, we selectively inhibited the most highly expressed subtypes. NF279 (P2X1-selective), 5-BDBD (P2X4-selective) and A804598 (P2X7-selective) were without effect, while NF157 (P2Y11/P2X1-selective) and NF340 (P2Y11-selective) significantly inhibited the ISO-promoted Ca^{2+} response (Figure 4C), suggesting a role for the P2Y11 purinergic receptor. The effect of NF449 (Figure 2A), NF340 and NF157 (Figure 4C) was specific to the β_2AR-stimulated response since these compounds did not significantly inhibit the carbamylcholine chloride (Cch)-stimulated increase in Ca^{2+} via endogenously expressed Gq-coupled muscarinic receptors in HA-β_2AR-HEK293S cells (Figures 4D). The effect of the P2Y11-selective antagonist, NF340, was concentration-dependent and resulted in a decrease in the E_{max} of the ISO-promoted Ca^{2+} response, with no significant effect on the EC_{50} (Figure 4E), confirming that its effect does not

Molecular Pharmacology Fast Forward. Published on March 9, 2017 as DOI: 10.1124/mol.116.106419
This article has not been copyedited and formatted. The final version may differ from this version.

occur directly through a competitive blockade of the β_2AR but instead suggesting a non-competitive antagonism of the response. Furthermore, both NF340 and NF157 were found to progressively decrease the ISO-promoted Ca^{2+} response in a dose-dependent manner, with potencies compatible with their affinity for the purinergic receptors (Figure 4F).

A previous study demonstrated that β_2AR activation could induce the release of adenine nucleotides from HEK293 cells (Sumi et al., 2010). To determine if the β_2AR promotes a Ca^{2+} response through the release of an extracellular mediator, leading to the subsequent transactivation of a purinergic receptor, we performed co-culture experiments in which parental HEK293S cells transfected with the obelin Ca^{2+} biosensor (obelin-HEK293S responder cells) were co-cultured at a 1:1 ratio with either parental HEK293S cells or with HA-β_2AR-HEK293S cells not expressing the biosensor (releaser cells). When obelin-HEK293S responders were co-cultured with releaser cells overexpressing the β_2AR (HA-β2AR-HEK293S), a significant potentiation in the Ca^{2+} response was observed following ISO treatment compared to co-culture with parental HEK293S releaser cells (Figure 5A), suggesting a role for the β_2AR-dependent release of an extracellular mediator acting in a paracrine manner. As a control experiment, we examined the Ca^{2+} response to Cch stimulation in both co-culture conditions and found no significant difference (Figure 5B), further supporting the β_2AR-specificity of this paracrine signalling response.

Since both ATP and ADP adenine nucleotides act as agonists for the P2Y11 receptor (van der Weyden et al., 2000), we assessed the role of extracellular adenine nucleotides in the β_2AR-promoted Ca^{2+} response, by pre-treating cells with apyrase, a cell-impermeable enzyme that hydrolyses both ATP and ADP to AMP. Apyrase treatment decreased both the efficacy (34% decrease in E_{max}) and potency (increase in EC_{50} from $9.2x10^{-8}$ M to $1.7x10^{-6}$ M) of the ISO-

Molecular Pharmacology Fast Forward. Published on March 9, 2017 as DOI: 10.1124/mol.116.106419
This article has not been copyedited and formatted. The final version may differ from this version.

promoted response (Figure 5C), consistent with the depletion of an extracellular mediator released upon β_2AR activation and acting in *trans* on the P2Y11 receptor. The Cch-mediated Ca^{2+} response, on the other hand, was not inhibited and instead was increased following apyrase treatment (Figure 5D). Consistent with adenine nucleotides being the paracrine mediator responsible for the transactivation, ISO treatment promoted the release of ATP from HA-β2AR-HEK293S cells (Figure 6A), with kinetics similar to those of the ISO-promoted Ca^{2+} response (reaching a maximum at 15 sec and returning to basal levels by 60 seconds). This ATP release was blocked by the β_2AR-selective antagonist, ICI 118,551, supporting a role for β2AR in the response (Figure 6B). These results are consistent with the hypothesis that β_2AR activation leads to the release of adenine nucleotides, which can act in *trans* on P2Y11 receptors to activate a Ca^{2+} response.

P2Y11 transactivation elicits a Gq-dependent increase in Ca^{2+} from intracellular stores: To investigate the potential role of Gq activation following P2Y11 transactivation (Qi et al., 2001), we tested the effects of overexpressing either WT Gαq or a dominant-negative mutant form of Gq (Gq-Q209L/D277N). Overexpression of WT Gq in HA-β_2AR-HEK293S cells increased the magnitude of the ISO-promoted Ca^{2+} response, whereas overexpression of Gq-Q209L/D277N or pre-treatment with the Gq-selective inhibitor FR900359 (Schrage et al., 2015) completely abolished the response (Figure 7). These results further support the involvement of a Gq-coupled receptor downstream of the β_2AR in the Ca^{2+} response.

We next assessed whether the increase in intracellular Ca^{2+} occurs via release from intracellular stores, as is typical for Gq-mediated responses. For this purpose, cells were pre-treated with the IP_3 receptor antagonist, 2-APB, the cell-permeable Ca^{2+} chelator, BAPTA-AM, or the sarco/endoplasmic reticulum Ca^{2+}-ATPase inhibitor, thapsigargin (TG). Upon stimulation

Molecular Pharmacology Fast Forward. Published on March 9, 2017 as DOI: 10.1124/mol.116.106419
This article has not been copyedited and formatted. The final version may differ from this version.

with ISO, the Ca^{2+} response was completely blocked by all three inhibitors (Figure 8A). These inhibitors had a similar effect on the Cch-mediated Ca^{2+} response, which activates a well-characterized IP_3-dependent pathway via activation of Gq-coupled muscarinic receptors (Caulfield, 1993) (Figure 8B). Together these data are consistent with the proposed transactivation of the Gq-coupled P2Y11 receptor upon activation of the β_2AR.

Molecular Pharmacology Fast Forward. Published on March 9, 2017 as DOI: 10.1124/mol.116.106419
This article has not been copyedited and formatted. The final version may differ from this version.

Discussion:

In this study, we describe a new node in the β_2AR signalling network involving a Gs-dependent but cAMP-independent release of ATP, which transactivates P2Y11 purinergic receptors and subsequently initiates a Gq-dependent mobilization of intracellular Ca^{2+}. This discovery is consistent with the accumulating reports that receptor transactivation, via the production and/or release of an extracellular mediator acting on a distal receptor, represents a *bona fide* signalling event for many GPCRs (Ostrom et al., 2000; Gschwind et al., 2001; Lee et al., 2002; Sumi et al., 2010). Given that the β_2AR and the P2Y receptors are co-expressed in various non-excitable tissues, including the brain, gastrointestinal tract, lung, adipocytes, kidney, skeletal muscle, heart and liver (Andre et al., 1996; Nicholas et al., 1996; Moore et al., 2001), the results obtained in the current study could provide additional insight into how β_2AR and P2Y receptors might collaborate in normal conditions and pathophysiology.

In addition to characterizing a new signalling modality for the β2AR, the present study introduces a new genetically engineered HEK293 cell line lacking both members of Gs (Gs and G_{olf}), offering a powerful tool to directly assess the contribution of Gs to cellular event. Current methods to investigate the role of Gs involve either overnight treatment with CTX, which initially causes chronic activation of Gs to stimulate its downregulation, the use of the few currently available small molecule inhibitors, which provide poor target specificity, and/or inhibition of the downstream effectors AC or protein kinase A. Genetic knockout of Gs provides a useful tool to specifically investigate the role of Gs and, as was the case in the present study, allow the discovery of Gs-dependent responses that do not require cAMP production. These cells should prove useful in future studies to explore additional non-canonical Gs signalling pathways.

Molecular Pharmacology Fast Forward. Published on March 9, 2017 as DOI: 10.1124/mol.116.106419
This article has not been copyedited and formatted. The final version may differ from this version.

Although the β_2AR-mediated release of adenine nucleotides has been described previously (Baker et al., 2004; Sumi et al., 2010), the functional consequences of this signalling event are just beginning to be explored. P2Y11 mRNA was the most abundant in HEK293S cells and it has the highest affinity for ATP compare to other purinergic receptors expressed in these cells (von Kügelgen et al., 2006). Yet, the capacity of the β_2AR to stimulate the release of ATP may in fact lead to the activation of other purinergic receptor subtypes in cells expressing a different repertoire or spatial organization of receptors.

The mechanism described in this study differs from previous reports of β_2AR-mediated Ca^{2+} responses in non-excitable HEK293 cells, which suggested a cAMP-dependent increase in intracellular Ca^{2+}, through a mechanism involving exchange protein directly activated by cAMP (EPAC) and phospholipase Cε or calcium release activated calcium (CRAC) channels (Schmidt et al., 2001; Keller et al., 2014). Although we cannot exclude a contribution of these mechanisms to the Ca^{2+} response studied here, our data clearly indicate that β_2AR activation in HEK293 cells can elicit a Ca^{2+} response independently of cAMP since blocking approximately 50% of the cAMP production did not affect the Ca^{2+} response (Figure 3A,B). Moreover, direct elevation of cAMP following treatment with forskolin or the cAMP analogue 8-Br-cAMP elicited only marginal Ca^{2+} responses compared to β_2AR stimulation (Figure 3D,E). Whether CRAC could subsequently contribute to the response following the initial Ca^{2+} mobilisation from the ER pool described in the current study has not been investigated. Interestingly, these previous studies used the Fura-2 indicator dye to measure intracellular Ca^{2+}, which is dissolved in the non-ionic detergent pluronic F127. This detergent inhibits the multi-drug resistant proteins (ABC-B transporters), which have been implicated in ATP transport to the extracellular space (Guan et al., 2011). The use of the genetically encoded obelin Ca^{2+} biosensor in the current study should

Molecular Pharmacology Fast Forward. Published on March 9, 2017 as DOI: 10.1124/mol.116.106419
This article has not been copyedited and formatted. The final version may differ from this version.

not interfere with this ATP release mechanism and may have aided in the elucidation of the mechanism described in the current work.

This collaboration between the β_2AR and purinergic receptors may be of particular relevance in the context of the airway epithelium. Indeed, the β_2AR plays an important role in the cAMP-dependent secretion of airway surfactants, ciliary beating and regulation of mucosal clearance (Wright and Dobbs, 1991; Salathe, 2002), properties that contribute to the therapeutic success of β_2AR agonists for the treatment of asthma (Giembycz and Newton, 2006). Interestingly, activation of Gq-coupled receptors and increases in intracellular Ca^{2+} promote undesirable inflammatory responses in pulmonary tissues (Barnes, 1998; Rider et al., 2011). Furthermore, an increase in purine nucleotide release from the airway epithelium is a hallmark of inflammatory diseases in the lungs (Burnstock et al., 2012) and purinergic signalling has been proposed to participate in asthmatic airway inflammation (Basoglu et al., 2005; Idzko et al., 2007) as well as in the pathogenesis of chronic obstructive pulmonary disorder (COPD) (Adriaensen and Timmermans, 2004; Mortaz et al., 2010). Given the beneficial effects of cAMP production and deleterious consequences of increases in intracellular Ca^{2+} in airway epithelia, the identification of functionally selective β_2AR ligands that stimulate cAMP production without promoting Ca^{2+} mobilization could represent a desirable class of β_2AR agonists for the treatment of pulmonary disorders. Salmeterol, a clinically effective β_2AR agonist used in the treatment of asthma, exhibits less side effects than what is typically associated with chronic use of other β_2AR agonists (Cazzola et al., 2013). Biased signalling studies have also shown that salmeterol is highly efficacious towards cAMP production but does not increase intracellular Ca^{2+} (van der Westhuizen et al., 2014). Given the results obtained in the current work, future studies examining the influence of purinergic receptor transactivation in the context of β_2AR-targeted treatment of

Molecular Pharmacology Fast Forward. Published on March 9, 2017 as DOI: 10.1124/mol.116.106419
This article has not been copyedited and formatted. The final version may differ from this version.

pulmonary disorders could be of great interest. Indeed, it is tempting to speculate that optimal therapy for such pulmonary disorders might involve harnessing the therapeutic benefit of β-adrenergic-mediated cAMP/PKA activity while avoiding the pro-inflammatory effect of purinergic transactivation and subsequent Ca^{2+}-dependent signalling.

Our study demonstrates a novel "inside-out" pathway for the β_2AR, adding to its signalling repertoire the transactivation of purinergic receptors and stimulation of Ca^{2+} mobilization. Given the preponderance of data supporting such transactivation mechanisms for both the β_2AR and other GPCR family members, we propose that such "inside-out" signalling events are not rare occurrences and instead represent a common signalling motif for GPCRs that may provide tissue-specific signalling in cells expressing a given repertoire of receptors.

Molecular Pharmacology Fast Forward. Published on March 9, 2017 as DOI: 10.1124/mol.116.106419
This article has not been copyedited and formatted. The final version may differ from this version.

Acknowledgements:

a) The authors would like to thank Dr. Monique Lagacé for critical reading of the manuscript. We would also like to thank Dr. Kumiko Makide and Yuji Shinjo for technical assistant of flow cytometry cell isolation and Kouki Kawakami for Western blot analysis.

Molecular Pharmacology Fast Forward. Published on March 9, 2017 as DOI: 10.1124/mol.116.106419
This article has not been copyedited and formatted. The final version may differ from this version.

Authorship contributions:

Participated in research design: Stallaert, van der Westhuizen, Le Gouill, Bouvier

Conducted Experiments: Stallaert, van der Westhuizen, Schonegge, Plouffe, Hogue, Lukashova

Contributed to new reagents or analytical tools: Inoue, Ishida, Aoki, Le Gouill

Performed data analysis: Stallaert, van der Westhuizen, Schonegge, Plouffe, Hogue, Lukashova, Inoue, Bouvier

Wrote or contributed to the writing of the manuscript: Stallaert, van der Westhuizen, Inoue, Bouvier

References:

Adriaensen D and Timmermans JP (2004) Purinergic signalling in the lung: important in asthma and COPD? *Curr Opin Pharmacol* **4**:207-214.

Andre C, Erraji L, Gaston J, Grimber G, Briand P and Guillet JG (1996) Transgenic mice carrying the human beta 2-adrenergic receptor gene with its own promoter overexpress beta 2-adrenergic receptors in liver. *Eur J Biochem* **241**:417-424.

Baker JG, Hall IP and Hill SJ (2004) Temporal characteristics of cAMP response element-mediated gene transcription: requirement for sustained cAMP production. *Mol Pharmacol* **65**:986-998.

Barnes PJ (1998) Pharmacology of airway smooth muscle. *Am J Respir Crit Care Med* **158**:S123-132.

Basoglu OK, Pelleg A, Essilfie-Quaye S, Brindicci C, Barnes PJ and Kharitonov SA (2005) Effects of aerosolized adenosine 5'-triphosphate vs adenosine 5'-monophosphate on dyspnea and airway caliber in healthy nonsmokers and patients with asthma. *Chest* **128**:1905-1909.

Benitah JP, Alvarez JL and Gomez AM (2010) L-type Ca(2+) current in ventricular cardiomyocytes. *J Mol Cell Cardiol* **48**:26-36.

Bolstad BM, Irizarry RA, Astrand M and Speed TP (2003) A comparison of normalization methods for high density oligonucleotide array data based on variance and bias. *Bioinformatics* **19**:185-193.

Bommakanti RK, Vinayak S and Simonds WF (2000) Dual regulation of Akt/protein kinase B by heterotrimeric G protein subunits. *J Biol Chem* **275**:38870-38876.

Braun K, Rettinger J, Ganso M, Kassack M, Hildebrandt C, Ullmann H, Nickel P, Schmalzing G and Lambrecht G (2001) NF449: a subnanomolar potency antagonist at recombinant rat P2X1 receptors. *Naunyn Schmiedebergs Arch Pharmacol* **364**:285-290.

Burnstock G, Brouns I, Adriaensen D and Timmermans JP (2012) Purinergic signaling in the airways. *Pharmacol Rev* **64**:834-868.

Caulfield MP (1993) Muscarinic receptors--characterization, coupling and function. *Pharmacol Ther* **58**:319-379.

Cazzola M, Page CP, Rogliani P and Matera MG (2013) beta2-agonist therapy in lung disease. *Am J Respir Crit Care Med* **187**:690-696.

Christ T, Galindo-Tovar A, Thoms M, Ravens U and Kaumann AJ (2009) Inotropy and L-type Ca2+ current, activated by beta1- and beta2-adrenoceptors, are differently controlled by phosphodiesterases 3 and 4 in rat heart. *Br J Pharmacol* **156**:62-83.

Collins S, Cao W and Robidoux J (2004) Learning new tricks from old dogs: beta-adrenergic receptors teach new lessons on firing up adipose tissue metabolism. *Mol Endocrinol* **18**:2123-2131.

Daaka Y, Luttrell LM, Ahn S, Della Rocca GJ, Ferguson SS, Caron MG and Lefkowitz RJ (1998) Essential role for G protein-coupled receptor endocytosis in the activation of mitogen-activated protein kinase. *J Biol Chem* **273**:685-688.

De Blasi A (1990) Beta-adrenergic receptors: structure, function and regulation. *Drugs Exp Clin Res* **16**:107-112.

Duarte T, Menezes-Rodrigues FS and Godinho RO (2012) Contribution of the extracellular cAMP-adenosine pathway to dual coupling of beta2-adrenoceptors to Gs and Gi proteins in mouse skeletal muscle. *J Pharmacol Exp Ther* **341**:820-828.

Dubey RK, Gillespie DG, Mi Z and Jackson EK (2001) Endogenous cyclic AMP-adenosine pathway regulates cardiac fibroblast growth. *Hypertension* **37**:1095-1100.

Dubey RK, Mi Z, Gillespie DG and Jackson EK (1996) Cyclic AMP-adenosine pathway inhibits vascular smooth muscle cell growth. *Hypertension* **28**:765-771.

El-Ajouz S, Ray D, Allsopp RC, Evans RJ (2012) Molecular basis of selective antagonism of the P2X1 receptor for ATP by NF449 and suramin: contribution of basic amino acids in the cysteine-rich loop. *Br J Pharmacol*165:390-400

Galandrin S and Bouvier M (2006) Distinct signaling profiles of beta1 and beta2 adrenergic receptor ligands toward adenylyl cyclase and mitogen-activated protein kinase reveals the pluridimensionality of efficacy. *Mol Pharmacol* **70**:1575-1584.

Gales C, Rebois RV, Hogue M, Trieu P, Breit A, Hebert TE and Bouvier M (2005) Real-time monitoring of receptor and G-protein interactions in living cells. *Nat Methods* **2**:177-184.

Giembycz MA and Newton R (2006) Beyond the dogma: novel beta2-adrenoceptor signalling in the airways. *Eur Respir J* **27**:1286-1306.

Gschwind A, Zwick E, Prenzel N, Leserer M and Ullrich A (2001) Cell communication networks: epidermal growth factor receptor transactivation as the paradigm for interreceptor signal transmission. *Oncogene* **20**:1594-1600.

Guan Y, Huang J, Zuo L, Xu J, Si L, Qiu J and Li G (2011) Effect of pluronic P123 and F127 block copolymer on P-glycoprotein transport and CYP3A metabolism. *Arch Pharm Res* **34**:1719-1728.

Guimaraes S and Moura D (2001) Vascular adrenoceptors: an update. *Pharmacol Rev* **53**:319-356.

Hohenegger M, Waldhoer M, Beindl W, Boing B, Kreimeyer A, Nickel P, Nanoff C and Freissmuth M (1998) Gsalpha-selective G protein antagonists. *Proc Natl Acad Sci U S A* **95**:346-351.

Idzko M, Hammad H, van Nimwegen M, Kool M, Willart MA, Muskens F, Hoogsteden HC, Luttmann W, Ferrari D, Di Virgilio F, Virchow JC, Jr. and Lambrecht BN (2007) Extracellular ATP triggers and maintains asthmatic airway inflammation by activating dendritic cells. *Nat Med* **13**:913-919.

Jackson EK, Koehler M, Mi Z, Dubey RK, Tofovic SP, Carcillo JA and Jones GS (1996) Possible role of adenosine deaminase in vaso-occlusive diseases. *J Hypertens* **14**:19-29.

Kassack MU, Braun K, Ganso M, Ullmann H, Nickel P, Boing B, Muller G and Lambrecht G (2004) Structure-activity relationships of analogues of NF449 confirm NF449 as the most potent and selective known P2X1 receptor antagonist. *Eur J Med Chem* **39**:345-357.

Keller MJ, Lecuona E, Prakriya M, Cheng Y, Soberanes S, Budinger GR and Sznajder JI (2014) Calcium release-activated calcium (CRAC) channels mediate the beta(2)-adrenergic regulation of Na,K-ATPase. *FEBS Lett* **588**:4686-4693.

Kim J, Eckhart AD, Eguchi S and Koch WJ (2002) Beta-adrenergic receptor-mediated DNA synthesis in cardiac fibroblasts is dependent on transactivation of the epidermal growth factor receptor and subsequent activation of extracellular signal-regulated kinases. *J Biol Chem* **277**:32116-32123.

Law SF, Yasuda K, Bell GI and Reisine T (1993) Gi alpha 3 and G(o) alpha selectively associate with the cloned somatostatin receptor subtype SSTR2. *J Biol Chem* **268**:10721-10727.

Lee FS, Rajagopal R and Chao MV (2002) Distinctive features of Trk neurotrophin receptor transactivation by G protein-coupled receptors. *Cytokine Growth Factor Rev* **13**:11-17.

Lemieux S (2006) Probe-level linear model fitting and mixture modeling results in high accuracy detection of differential gene expression. *BMC Bioinformatics* **7**:391.

Levis MJ and Bourne HR (1992) Activation of the alpha subunit of Gs in intact cells alters its abundance, rate of degradation, and membrane avidity. *J Cell Biol* **119**:1297-1307.

Montalbetti N, Leal Denis MF, Pignataro OP, Kobatake E, Lazarowski ER and Schwarzbaum PJ (2011) Homeostasis of extracellular ATP in human erythrocytes. *J Biol Chem* **286**:38397-38407.

Moore DJ, Chambers JK, Wahlin JP, Tan KB, Moore GB, Jenkins O, Emson PC and Murdock PR (2001) Expression pattern of human P2Y receptor subtypes: a quantitative reverse transcription-polymerase chain reaction study. *Biochim Biophys Acta* **1521**:107-119.

Mortaz E, Folkerts G, Nijkamp FP and Henricks PA (2010) ATP and the pathogenesis of COPD. *Eur J Pharmacol* **638**:1-4.

Nicholas AP, Hokfelt T and Pieribone VA (1996) The distribution and significance of CNS adrenoceptors examined with in situ hybridization. *Trends Pharmacol Sci* **17**:245-255.

Ostrom RS, Gregorian C and Insel PA (2000) Cellular release of and response to ATP as key determinants of the set-point of signal transduction pathways. *J Biol Chem* **275**:11735-11739.

Perez-Schindler J, Philp A and Hernandez-Cascales J (2013) Pathophysiological relevance of the cardiac beta2-adrenergic receptor and its potential as a therapeutic target to improve cardiac function. *Eur J Pharmacol* **698**:39-47.

Qi AD, Kennedy C, Harden TK and Nicholas RA (2001) Differential coupling of the human P2Y(11) receptor to phospholipase C and adenylyl cyclase. *Br J Pharmacol* **132**:318-326.

Ran FA, Hsu PD, Wright J, Agarwala V, Scott DA and Zhang F (2013) Genome engineering using the CRISPR-Cas9 system. *Nat Protoc* **8**:2281-2308.

Reed SE, Staley EM, Mayginnes JP, Pintel DJ and Tullis GE (2006) Transfection of mammalian cells using linear polyethylenimine is a simple and effective means of producing recombinant adeno-associated virus vectors. *J Virol Methods* **138**:85-98.

Rider CF, King EM, Holden NS, Giembycz MA and Newton R (2011) Inflammatory stimuli inhibit glucocorticoid-dependent transactivation in human pulmonary epithelial cells: rescue by long-acting beta2-adrenoceptor agonists. *J Pharmacol Exp Ther* **338**:860-869.

Salathe M (2002) Effects of beta-agonists on airway epithelial cells. *J Allergy Clin Immunol* **110**:S275-281.

Schmidt M, Evellin S, Weernink PA, von Dorp F, Rehmann H, Lomasney JW and Jakobs KH (2001) A new phospholipase-C-calcium signalling pathway mediated by cyclic AMP and a Rap GTPase. *Nat Cell Biol* **3**:1020-1024.

Schrage R, Schmitz AL, Gaffal E, Annala S, Kehraus S, Wenzel D, Büllesbach KM, Bald T, Inoue A, Shinjo Y, Galandrin S, Shridhar N, Hesse M, Grundmann M, Merten N, Charpentier TH, Martz M, Butcher AJ, Slodczyk T, Armando S, Effern M, Namkung Y, Jenkins L, Horn V, Stößel A, Dargatz H, Tietze D, Imhof D, Galés C, Drewke C, Müller CE, Hölzel M, Milligan G, Tobin AB, Gomeza J, Dohlman HG, Sondek J, Harden TK, Bouvier M, Laporte SA, Aoki J, Fleischmann BK, Mohr K, König GM, Tüting T, Kostenis E (2015) The experimental power of FR900359 to study Gq-regulated biological processes. *Nat Commun* **6**:10156.

Seamon KB, Padgett W and Daly JW (1981) Forskolin: unique diterpene activator of adenylate cyclase in membranes and in intact cells. *Proc Natl Acad Sci U S A* **78**:3363-3367.

Sitkauskiene B and Sakalauskas R (2005) The role of beta(2)-adrenergic receptors in inflammation and allergy. *Curr Drug Targets Inflamm Allergy* **4**:157-162.

Stallaert W, Dorn JF, van der Westhuizen E, Audet M and Bouvier M (2012) Impedance responses reveal beta(2)-adrenergic receptor signaling pluridimensionality and allow classification of ligands with distinct signaling profiles. *PLoS One* **7**:e29420.

Sumi Y, Woehrle T, Chen Y, Yao Y, Li A and Junger WG (2010) Adrenergic receptor activation involves ATP release and feedback through purinergic receptors. *Am J Physiol Cell Physiol* **299**:C1118-1126.

van der Westhuizen ET, Breton B, Christopoulos A and Bouvier M (2014) Quantification of ligand bias for clinically relevant beta2-adrenergic receptor ligands: implications for drug taxonomy. *Mol Pharmacol* **85**:492-509.

van der Weyden L, Adams DJ, Luttrell BM, Conigrave AD and Morris MB (2000) Pharmacological characterisation of the P2Y11 receptor in stably transfected haematological cell lines. *Mol Cell Biochem* **213**:75-81.

von Kügelgen I (2006) Pharmacological profiles of cloned mammalian P2Y-receptor subtypes. *Pharmacol Ther* **110**:415-432.

Wright JR and Dobbs LG (1991) Regulation of pulmonary surfactant secretion and clearance. *Annu Rev Physiol* **53**:395-414.

Zhang ZS, Cheng HJ, Ukai T, Tachibana H and Cheng CP (2001) Enhanced cardiac L-type calcium current response to beta2-adrenergic stimulation in heart failure. *J Pharmacol Exp Ther* **298**:188-196.

Molecular Pharmacology Fast Forward. Published on March 9, 2017 as DOI: 10.1124/mol.116.106419
This article has not been copyedited and formatted. The final version may differ from this version.

Footnotes:

a) This work was supported, in part, by grants from the Canadian Institutes for Health Research (CIHR) [MOP 11215] to MB, PRESTO, JST to AI and AMED-CREST, AMED to JA. WS was supported by the Vanier Canada Graduate Scholarship from the CIHR. ETvdW was supported by post-doctoral research fellowships from the CIHR, the Canadian Hypertension Society, the Fonds de la Recherche en Santé du Quebec (FRSQ) and the National Health and Medical Research Council Australia (NHMRC) [GNT-1013819]. A-MS was supported by post-doctoral research fellowships from the FRSQ while BP was supported by post-doctoral research fellowships from the CIHR. MB holds the Canada Research Chair in Signal Transduction and Molecular Pharmacology.

b)

c) Reprint requests to: Michel Bouvier, IRIC - Université de Montréal, P.O. Box 6128 Succursale Centre-Ville, Montréal, Qc. Canada, H3C 3J7. Email: michel.bouvier@umontreal.ca

d) WS and ETvdW contributed equally to this work.

Molecular Pharmacology Fast Forward. Published on March 9, 2017 as DOI: 10.1124/mol.116.106419
This article has not been copyedited and formatted. The final version may differ from this version.

Figure legends:

Figure 1 – Isoproterenol increases intracellular Ca^{2+} via the β_2AR. HEK293S (endogenously expressing β_2AR at 18.74±3.14 fmol/mg protein) or HA-β_2AR-HEK293S (stably expressing β_2AR at 3 174±320 fmol/mg protein) cells were transiently transfected with mCherry-obelin. (A-B) Cells were treated with vehicle or isoproterenol (ISO; 10 μM) and increases in intracellular Ca^{2+} (increases in obelin relative luminescence unit, RLU) were measured. (C) Cells were pre-treated with vehicle (Ctl) or ICI 118,551 (ICI, 100 nM) for 1 h, then treated with ISO (10 μM). Data represent ISO-promoted peak Ca^{2+} responses. (D) The Ca^{2+} response was measured with increasing concentrations of ISO. EC_{50} values: 7.32±0.10 for HEK293S and 7.05±0.16 for HA-β_2AR-HEK293S. Data are expressed as the mean ± S.E.M. of 3-4 independent experiments, each performed in triplicate. Data in column graphs were analyzed by two-tailed paired Student's t-test, where $p<0.05$ (*) was considered significant.

Figure 2 – The ISO-promoted increase in intracellular Ca^{2+} is Gs-dependent. (A) HA-β_2AR-HEK293S cells transiently transfected with mCherry-obelin were pre-treated with cholera toxin (CTX) (200 ng/ml; 18 h) or with NF449 (10 μM; 1 h). Cells were treated with isoproterenol (ISO; 10 μM) and increases in intracellular Ca^{2+} were measured. *Inset:* The area under the curve (AUC) was calculated for each treatment. (B) HA-β_2AR-HEK293S cells were transiently transfected with Gαs-67-RlucII and GFP_{10}-Gγ1. Cells were pre-treated with vehicle (Ctl), CTX or NF449, as indicated above, followed by ISO treatment, and Gs activation was measured as a decrease in the BRET response. Protein extracts from parental HEK293 and three clones of ΔGs-HEK293 cells were separated on SDS-PAGE and immunoblotted with anti-Gαs/olf antibody (top

Molecular Pharmacology Fast Forward. Published on March 9, 2017 as DOI: 10.1124/mol.116.106419
This article has not been copyedited and formatted. The final version may differ from this version.

panel) or anti-α-tubulin antibody (bottom panel). Note that the parental HEK293 cells express the long (GαsL) and short (GαsS) Gαs isoforms while they were both undetectable in the mutant clones. (D) The parental HEK293 or ΔGs-HEK293 (Clone1) cells were transiently transfected with GFP_{10}-EPAC-R*luc*II. Cells were then treated with either isoproterenol (ISO; 10 μM) or forskolin (Fsk; 10 μM) for 20 min. ISO increased intracellular cAMP levels in HEK293 cells at a similar level to Fsk while the response to ISO was significantly blocked in ΔGs-HEK293 cells. (E-F) The parental HEK293 or ΔGs-HEK293 (Clone1) cells were transiently transfected with β2AR and Obelin-GFP2, and treated with ISO (10μM, C) or the Ca^{2+} ionophore A23187 (10 μM, D). ISO increased intracellular Ca^{2+} in the parental HEK293 cells while the response was blocked in ΔGs-HEK293 cells (E). The response to the Ca^{2+} ionophore A23187 was comparable in both cells lines (F). cAMP and Ca^{2+} data for the 2 other clones are shown in Supplemental Figure 4. Data are expressed as the mean ± S.E.M. of 3-6 independent experiments, each performed in duplicate or triplicate. Data in panel A were analyzed by one-way ANOVA, with a Dunnett's multiple comparison *post-hoc* test, where $p<0.05$ (*) was considered significant. Data in planel D were analyzed by two-way ANOVAbfollowed by a Sidak's multiple comparison *post-hoc* test, where $p<0.05$ (*) and $p<0.001$ (***)was considered significant.

Figure 3 – The ISO-promoted increase in Ca^{2+} is independent of cAMP production. (A) HA-β_2AR-HEK293S cells were pretreated with vehicle or the adenylyl cyclase inhibitor, SQ22536 (100 mM, 1 h), then treated with isoproterenol (ISO; 10 μM) and cAMP measured using the Cisbio kit. (B-E) HA-β_2AR-HEK293S cells were transiently transfected with either GFP_{10}-EPAC-vYFP (C) or mCherry-obelin (B, D-E). (B) Cells were treated as in A and Ca^{2+} response measured. *Inset:* Ca^{2+} response was plotted using the area under the curve (AUC).

Molecular Pharmacology Fast Forward. Published on March 9, 2017 as DOI: 10.1124/mol.116.106419
This article has not been copyedited and formatted. The final version may differ from this version.

SQ22536 significantly inhibited ISO-promoted cAMP production, but did not attenuate the ISO-induced Ca^{2+} response. (C-D) Cells were treated with either forskolin (Fsk; 100 μM, 30 min) or ISO and cAMP (C) and Ca^{2+} (D) responses were measured. Fsk activates cAMP production to a similar extent as ISO (C), but stimulates only a marginal Ca^{2+} response compared to ISO (D) and over vehicle (D, inset). (E) Cells were stimulated or not (vehicle) with ISO or the non-hydrolysable cAMP analog, 8-bromo-cAMP (100 μM) and Ca^{2+} response measured. *Inset:* Ca^{2+} response was plotted using the area under the curve (AUC). Data are expressed as the mean ± S.E.M. of 3-6 independent experiments, each performed in duplicate or triplicate. Column graphs were analyzed by two-tailed paired Student's t-tests, where $p<0.05$ (*) was considered significant.

Figure 4 – The ISO-promoted Ca^{2+} response is inhibited upon purinergic receptor blockade. (A-E) HA-β_2AR-HEK293S cells transiently transfected with mCherry-obelin were pretreated with the pan-adenosine receptor antagonist CGS15943 (1 μM, 30 min) (B) or the purinergic receptor antagonists: suramin (500 μM; 1 h) (A, C), NF279 (1 μM, 30 min) (C), 5-BDBD (10 μM, 30 min) (C), A804598 (1 μM, 30 min) (C), NF449 (10 μM, 30 min) (D), NF157 (10 μM, 30 min) (C-D) or NF340 (10 μM, 30 min) (C-D). Cells were then stimulated with either ISO (10 μM) (A-C, E) or Carbamylcholine chloride (Cch, 100 μM) (D), and the Ca^{2+} response was measured. *Inset in A and B* shows the Ca^{2+} response plotted using the area under the curve (AUC). (E) Cells were pre-treated with vehicle (Ctl) or the indicated concentration of NF340, followed by stimulation with increasing concentrations of ISO and the Ca^{2+} response was measured. (F) Cells were pretreated with increasing concentration of either NF157 or NF340, followed by stimulation with ISO at an EC_{80} concentration (150 nM). Ca^{2+} response was then

Molecular Pharmacology Fast Forward. Published on March 9, 2017 as DOI: 10.1124/mol.116.106419
This article has not been copyedited and formatted. The final version may differ from this version.

measured. IC_{50} values: 4.36 ± 1.91 μM for NF157 and 50.4 ± 27.5 μM for NF340. Data are expressed as the mean ± S.E.M. of 3-4 independent experiments, each performed in triplicate. Area under the curve (AUC) data presented in column graphs were analyzed by two-tailed unpaired Student's t-tests, where $p<0.05$ (*) was considered significant.

Figure 5 – ISO stimulates the releases of an extracellular mediator involved in the Ca^{2+} response. Parental HEK293S cells were transiently transfected with mCherry-obelin and co-cultured with HEK293S or HA-β_2AR-HEK293S cells not expressing the biosensor. (A-B) Cells were treated with either ISO (10 μM) (A) or Cch (100 μM) (B) and the Ca^{2+} response was measured. (C-D) Cells were pre-treated with apyrase (1 UI/ml; 1 h) followed by stimulation with increasing concentration of ISO (C) or Cch (100 μM) (D) and the Ca^{2+} response was measured. *Inset for A, B and D*: Ca^{2+} response plotted using the area under the curve (AUC). Data are expressed as the mean ± S.E.M. of 3 independent experiments, each performed in triplicate. Area under the curve (AUC) data presented in column graphs were analyzed by two-tailed paired t-tests, where $p<0.05$ (*) was considered significant.

Figure 6 – ISO promotes ATP release in HA-β_2AR-HEK293S cells. HA-β2AR-HEK293S cells were stimulated with ISO (10 μM) for different time points and ATP was measured in the bulk media. (A) ISO promoted a rapid and transient release of ATP over a period of 60 sec, with peak release measured at 30 sec. (B) The response to ISO was blocked in both HEK293S and HA-β2AR-HEK293S cells pre-treated with the β2AR-selective antagonist ICI 118551. Data are the mean ± S.E.M. of 2-4 independent experiments performed in duplicate.

Molecular Pharmacology Fast Forward. Published on March 9, 2017 as DOI: 10.1124/mol.116.106419
This article has not been copyedited and formatted. The final version may differ from this version.

Figure 7 – The ISO-promoted Ca^{2+} response is modulated by wild-type or dominant negative Gq overexpression. HA-β_2AR-HEK293S were transiently transfected or not (Mock) with either wild-type Gq or a dominant negative mutant of Gq (Q209L/D277N) (Gq-DN), or pre-treated with the Gq-selective inhibitor FR900359, and the Ca^{2+} response was measured. Data are expressed as the mean ± S.E.M. of 4-5 independent experiments, each performed in triplicate.

Figure 8 – Ca^{2+} originating from the intracellular stores is involved in the ISO and Cch-mediated responses. HA-β_2AR-HEK293S cells were pre-treated with the sarco/endoplasmic reticulum Ca^{2+}-ATPase inhibitor thapsigargin (Tg; 5 μM, 1 h), the cell-permeable Ca^{2+} chelator BAPTA-AM (20 μM, 1 h), or the IP_3 receptor antagonist 2-aminoethoxydiphenyl borate (2-APB; 200 μM, 1 h), followed by stimulation with ISO (10 μM) (A) or Cch (100 μM) (B) and the Ca^{2+} response was measured. *Inset for A and B*: Ca^{2+} response plotted using the area under the curve (AUC). Data are expressed as the mean ± S.E.M. of 3-6 independent experiments, each performed in triplicate. Area under the curve (AUC) data in column graphs were analyzed by one-way ANOVA, with a Dunnett's multiple comparison *post-hoc* test, where $p<0.05$ (*) was considered significant.

Molecular Pharmacology Fast Forward. Published on March 9, 2017 as DOI: 10.1124/mol.116.106419
This article has not been copyedited and formatted. The final version may differ from this version.

FIGURE 1

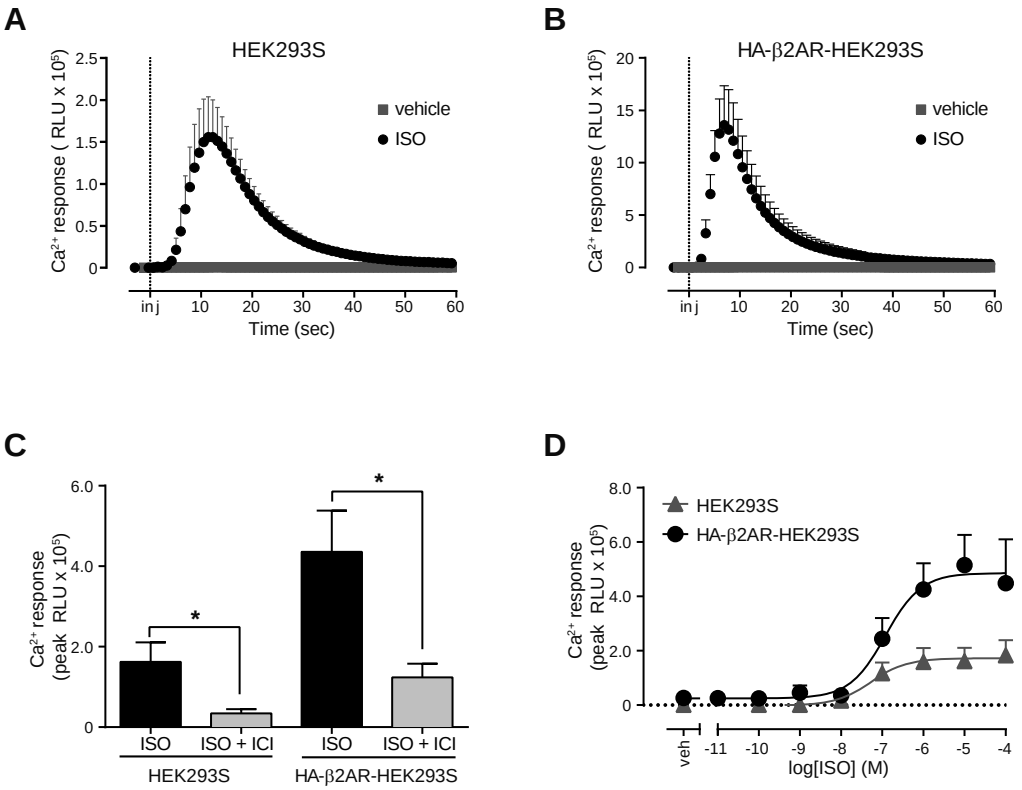

Molecular Pharmacology Fast Forward. Published on March 9, 2017 as DOI: 10.1124/mol.116.106419
This article has not been copyedited and formatted. The final version may differ from this version.

FIGURE 2

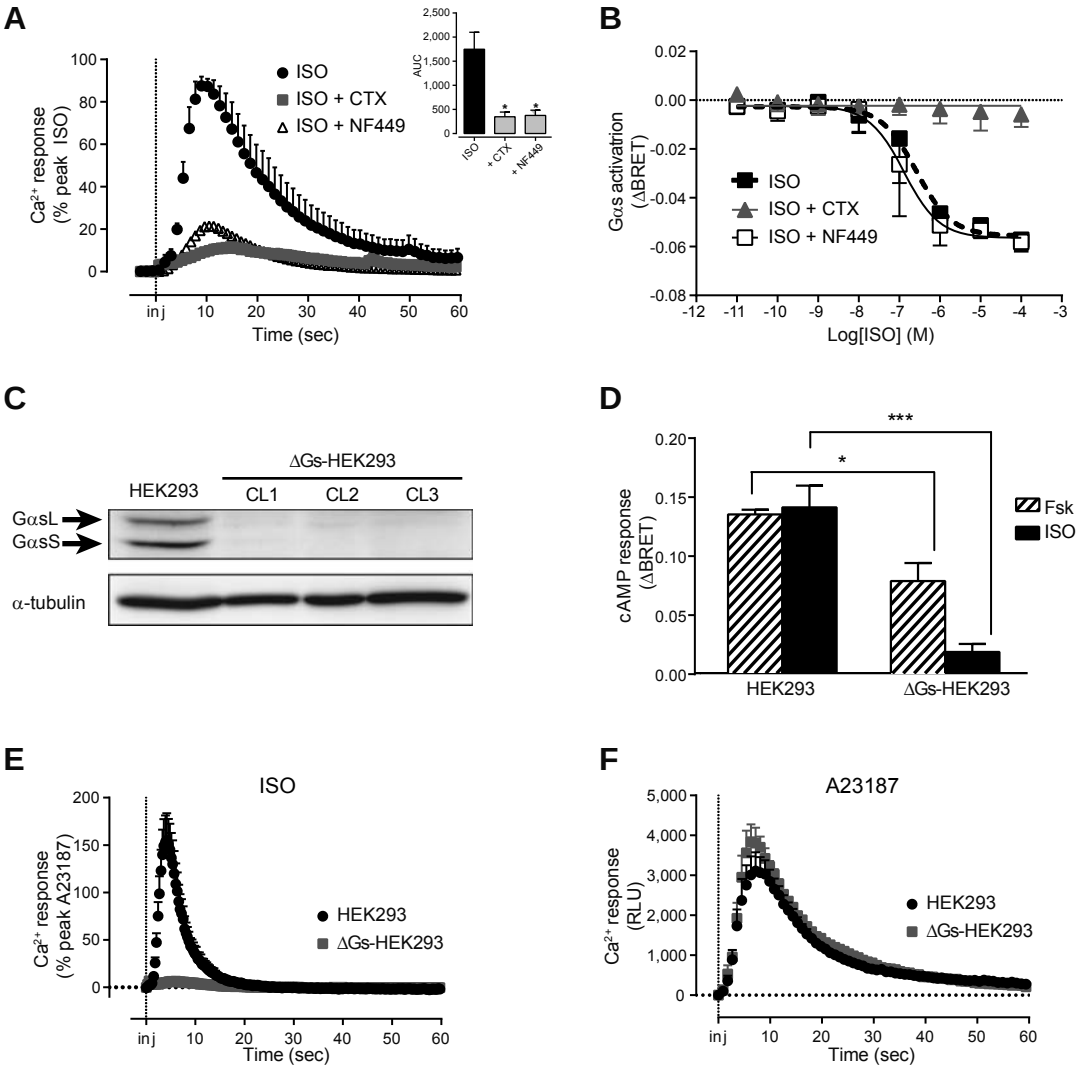

Molecular Pharmacology Fast Forward. Published on March 9, 2017 as DOI: 10.1124/mol.116.106419
This article has not been copyedited and formatted. The final version may differ from this version.

FIGURE 3

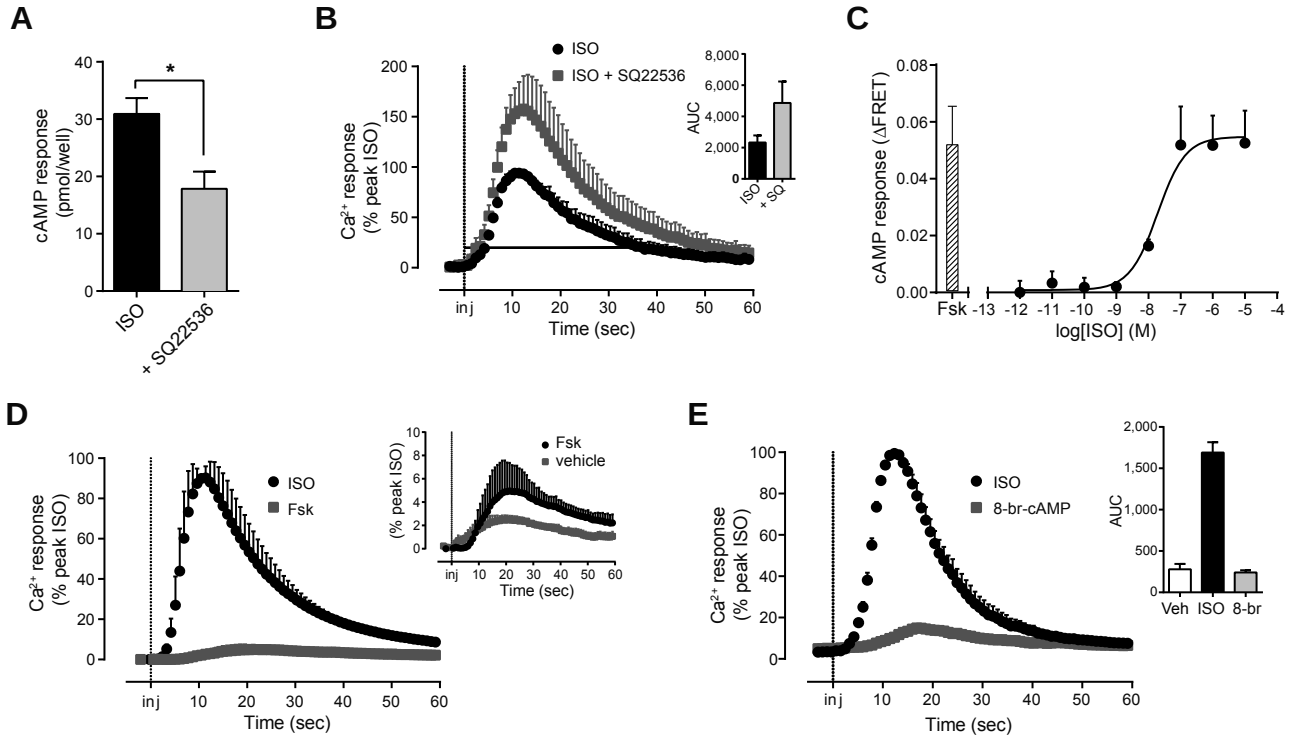

Molecular Pharmacology Fast Forward. Published on March 9, 2017 as DOI: 10.1124/mol.116.106419
This article has not been copyedited and formatted. The final version may differ from this version.

FIGURE 4

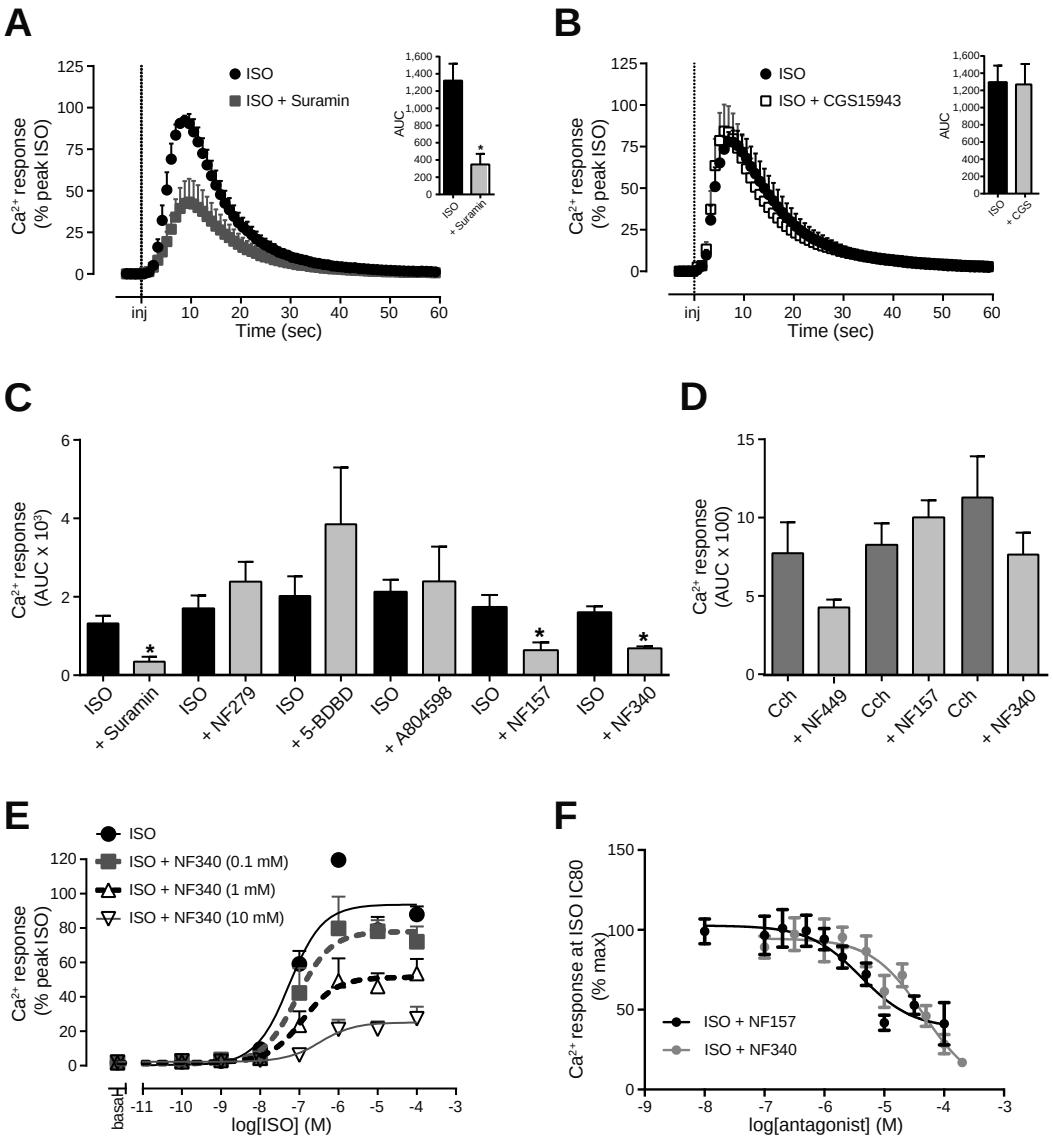

Molecular Pharmacology Fast Forward. Published on March 9, 2017 as DOI: 10.1124/mol.116.106419
This article has not been copyedited and formatted. The final version may differ from this version.

FIGURE 5

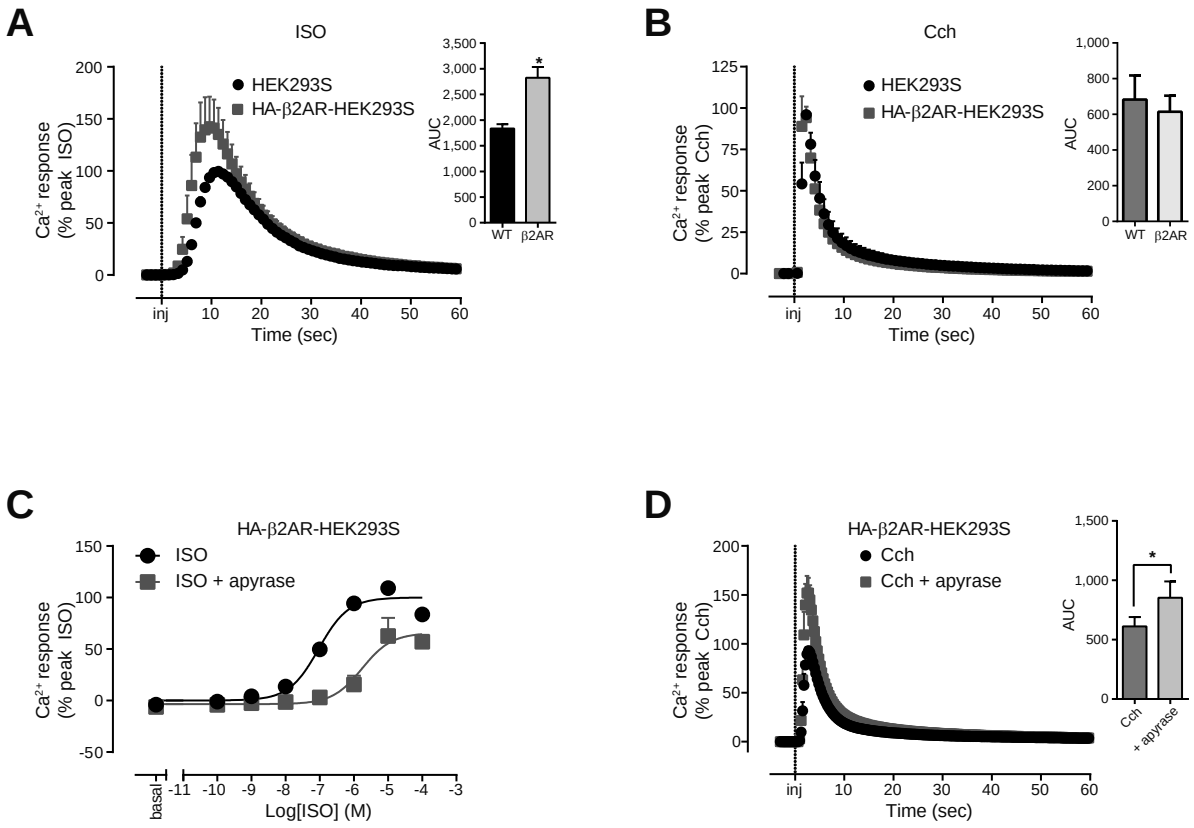

Molecular Pharmacology Fast Forward. Published on March 9, 2017 as DOI: 10.1124/mol.116.106419
This article has not been copyedited and formatted. The final version may differ from this version.

FIGURE 6

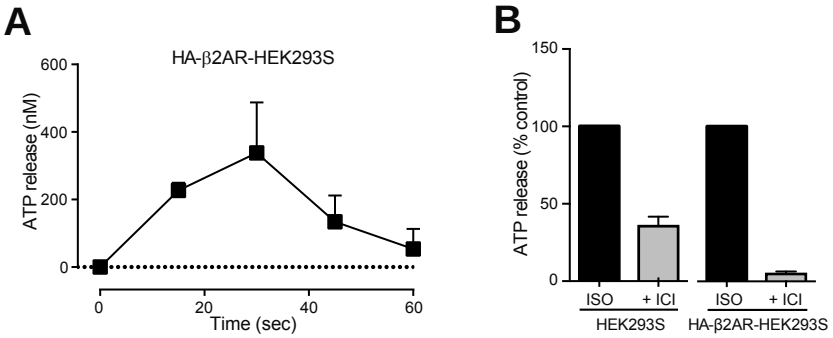

Molecular Pharmacology Fast Forward. Published on March 9, 2017 as DOI: 10.1124/mol.116.106419
This article has not been copyedited and formatted. The final version may differ from this version.

FIGURE 7

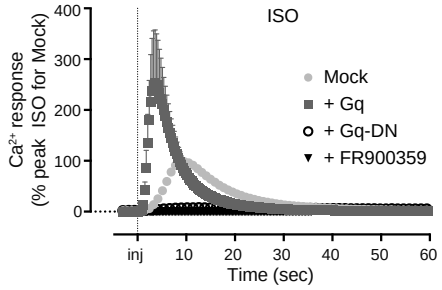

Molecular Pharmacology Fast Forward. Published on March 9, 2017 as DOI: 10.1124/mol.116.106419
This article has not been copyedited and formatted. The final version may differ from this version.

FIGURE 8